ARTICLE

Check for updates

High rates of daytime river metabolism are an underestimated component of carbon cycling

Flavia Tromboni [1,2✉], Erin R. Hotchkiss [3], Anne E. Schechner[2,4], Walter K. Dodds [4], Simon R. Poulson[5] & Sudeep Chandra [1]

River metabolism and, thus, carbon cycling are governed by gross primary production and ecosystem respiration. Traditionally river metabolism is derived from diel dissolved oxygen concentrations, which cannot resolve diel changes in ecosystem respiration. Here, we compare river metabolism derived from oxygen concentrations with estimates from stable oxygen isotope signatures ($\delta^{18}O_2$) from 14 sites in rivers across three biomes using Bayesian inverse modeling. We find isotopically derived ecosystem respiration was greater in the day than night for all rivers (maximum change of $113\,g\,O_2\,m^{-2}\,d^{-1}$, minimum of $1\,g\,O_2\,m^{-2}\,d^{-1}$). Temperature (20 °C) normalized rates of ecosystem respiration and gross primary production were 1.1 to 87 and 1.5 to 22-fold higher when derived from oxygen isotope data compared to concentration data. Through accounting for diel variation in ecosystem respiration, our isotopically-derived rates suggest that ecosystem respiration and microbial carbon cycling in rivers is more rapid than predicted by traditional methods.

[1] Global Water Center and Department of Biology, University of Nevada Reno, Reno, NV 89557, USA. [2] Leibniz Institute of Freshwater Ecology and Inland Fisheries, Berlin, Germany. [3] Department of Biological Sciences, Virginia Polytechnic Institute and State University, Blacksburg, VA, USA. [4] Division of Biology, Kansas State University, Manhattan, KS 66506, USA. [5] Global Water Center and Department of Geological Sciences and Engineering, University of Nevada Reno, Reno, NV 89557, USA. ✉email: ftromboni@unr.edu

R ivers play an important role in global carbon cycling and climate regulation, as they actively retain, transform, and release carbon[1–3]. River ecosystem metabolism includes two processes, carbon fixation (Gross Primary Production—GPP) and mineralization (Ecosystem Respiration—ER), which reflect the sources and cycling of energy within a stream[4]. Metabolism measurements in rivers have become more widely available[5] and have been used across the globe to evaluate aquatic ecosystem responses to environmental change[6–8]. In general, river metabolism varies globally as a function of climate, elevation, and latitude[9].

Accurate assessment of an ecosystem's carbon fluxes requires an understanding of the magnitude of GPP and ER (i.e., metabolism) as well as the processes that govern metabolic rates. Most metabolism modeling approaches use measurements from diel dissolved oxygen (O_2) concentrations and C:O stoichiometry to estimate carbon flux, and assume that estimates of nighttime ER also apply to daytime ER[10]. However, analyzing $\delta^{18}O_2$ across day and night allows for tracking within-day changes in ER, as respiration preferentially takes up the lighter ^{16}O isotope and enriches $^{18}O_2$ relative to $^{16}O_2$ in the water. In contrast, photosynthesis produces $\delta^{18}O_2$ values that match the $\delta^{18}O_2$ composition of the water[11], while gas exchange of O_2 with the atmosphere shifts $\delta^{18}O_2$ values towards equilibrium with atmospheric O_2[11]. Measuring changes in $\delta^{18}O_2$ throughout 24-h (i.e., diel) periods can thus help ecosystem scientists assess diel ER patterns without the confounding effect of GPP[12–15].

Modeling approaches that include $\delta^{18}O_2$ values from field measurements are rarely applied. Previous studies have reported diel changes of dissolved $\delta^{18}O_2$ and dissolved inorganic carbon[16,17] but did not leverage isotopic fractionation of O_2 during respiration to estimate changes in ER over diel cycles. Additional investigations developed models using both O_2 concentrations and $\delta^{18}O_2$ values to model daily rates of GPP and ER and estimated diel changes in ER based on diel temperature variation[14,18], finding higher daily ER rates compared to modeled estimates from O_2 concentrations alone.

A few prior studies have assessed diel changes in metabolism using ambient changes in $\delta^{18}O_2$. Research from one lake[19] and one marine ecosystem[20] using $\delta^{18}O_2$ to estimate daytime patterns of ER showed that is underestimated with traditional O_2-only models. In rivers, two studies representing four streams[13,15] used modeling approaches that included diel $\delta^{18}O_2$ data, indicating that daytime ER increased up to 30% relative to nighttime ER in one productive stream in the midwestern United States[13] and by up to 340% in three streams in Wyoming (U.S.)[15]. These results suggest that traditional metabolism estimates based on O_2 concentration alone could underestimate both ER and GPP, potentially mischaracterizing important ecosystem carbon fluxes and their environmental controls over 24-h periods. However, these two studies are limited to productive streams in temperate regions of the United States and did not include larger rivers or multiple globally relevant biomes.

Prior research has not specifically explored factors that might lead to higher estimated daytime ER based on $\delta^{18}O_2$ data in flowing waters and are not extensive enough to understand the magnitude and generality of higher daytime ER across a variety of ecosystem sizes and biomes. River and stream metabolism rates obtained with traditional, diel O_2 methods suggest that GPP and ER vary with ecosystem size, climate, land-use, and local scale variation[21,22]. Consequently, understanding a broad range of variation in diel ER in streams and rivers spanning a gradient of productivity and other environmental characteristics, outside of four streams in the temperate United States, is warranted.

Several mechanisms may explain why ER can be greater during the day related to factors that influence benthic biofilms (the site of highest metabolic activity in most streams and rivers). First, photosynthetic organisms provide reactive organic carbon compounds to heterotrophic microbes (i.e., the microbial loop) by releasing dissolved organic carbon exudates while photosynthesizing during the day[23,24]. Second, organic carbon may support daytime heterotrophic activity due to photolysis of carbon increasing bioavailability[25,26]. Third, higher water temperatures during the day could increase metabolic activity of organisms (models tying metabolic rates to temperature fit diurnal O_2 patterns better than those that do not[27,28]). Fourth, increased temperatures could drive changes in water viscosity and in the thickness of the diffusion boundary layer at the biofilm interface, leading to changes in diffusion limitations and thus changes in isotopic fractionation[29,30]. Finally, photorespiration could be stimulated with high light, high temperature, and other factors that lead to higher O_2 concentrations relative to CO_2 in cells responsible for CO_2 fixation. This leads to an increase in the rate at which RuBisCO oxygenates RuBP and leads to rapid cycling of O_2 without corresponding CO_2 fixation[31,32].

We characterized how metabolism estimates from traditional and most commonly used O_2-only models that assume constant or temperature-driven rates of ER, vary from those made by assessing diel variations of $\delta^{18}O_2$ in discrete samples in addition to sensing changes in O_2 logged with diurnal sensors. We estimated metabolism in fourteen sites located in rivers in different ecoregions and biomes (subarctic, tropical, and temperate) to capture a broad diversity of climatic zones, productivity, and river size. We use data and model results from these rivers to address the following questions: How much does diel ER vary in rivers across the globe? What drives diel variation in metabolism? Is daytime ER higher due to greater carbon availability to heterotrophs during photosynthesis? We predicted that if diel temperature changes drive variation in ER rates more so than diel changes in carbon substrates from GPP, we should see less discrepancy between day and night ER in tropical (relatively constant water temperature) than in temperate rivers. We used regression analysis to assess factors that might have influenced diel ER across widely distributed ecosystems.

We found that rivers have substantially higher daytime ER than nighttime throughout all ecoregions and biomes, which begins to address the knowledge gap in our understanding of diel metabolic patterns in running waters based on prior studies that include only four productive temperate streams. We rule out some potential explanations for our observations leading us to propose daytime ER is a traditionally underestimated component of riverine carbon cycling and find it likely that the riverine microbial loop cycles carbon faster than previously thought.

Results

Ecosystem metabolism characteristics from O_2 concentration and isotopic composition. All rivers were heterotrophic (ER>GPP) apart from the Sekong river in Cambodia, which was autotrophic, as assessed with the traditional diel O_2 metabolism models as well as $\delta^{18}O_2$ models (Supplementary Table 1 and Fig. 1). Net ecosystem production (NEP) ranged from -10.1 g O_2 m^{-2} d^{-1} in the Tensleep river in the Mountain Steppe, to 0.5 g O_2 m^{-2} d^{-1} in the tropical Sekong (NEP = GPP -|ER|, where modeled ER values are negative because they are consuming O_2). In this paper, we will refer to GPP_{O_2} and ER_{O_2} when metabolism estimates are from the traditional model based on diel O_2 concentration only (Eq. (3)), and $\delta^{18}O_2$-GPP and $\delta^{18}O_2$-ER when they result from the $\delta^{18}O_2$ and O_2 paired models that estimate the model parameter dielMET in addition to $\delta^{18}O_2$-GPP and $\delta^{18}O_2$-ER (Eqs. (4a) and (4b)).
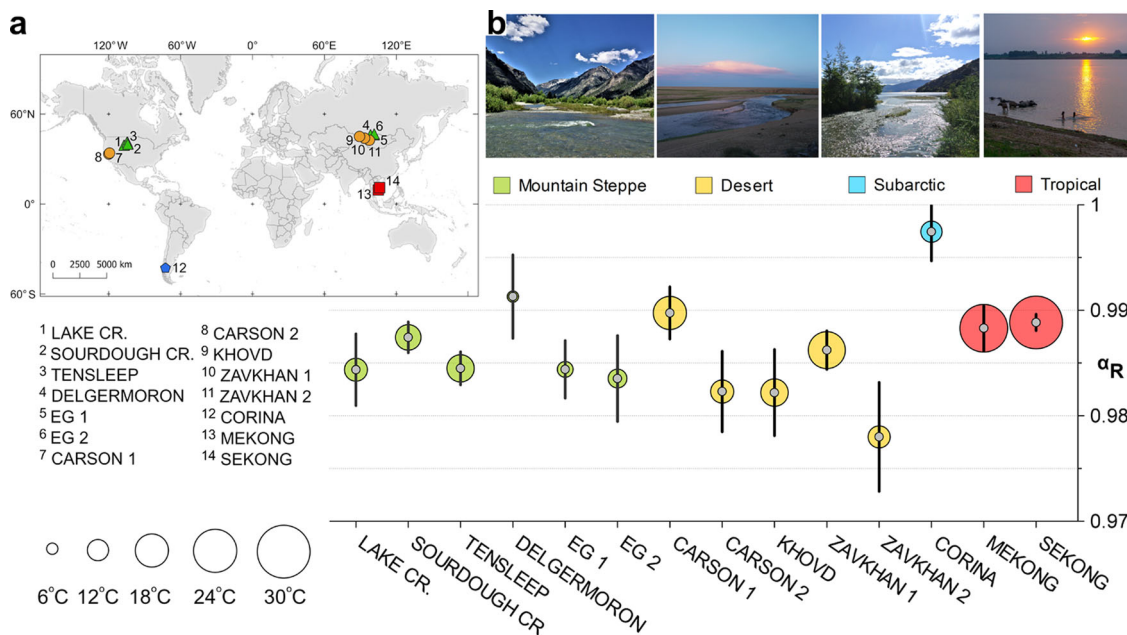
Fig. 1 Map of study sites of different biomes and isotopic fractionation factor (α_R) values tested in the models. a Map using green triangles to note temperate river sites, yellow circles for desert sites, red squares for tropical sites, and a blue pentagon for the sub-arctic site. **b** Gray dots represent average measured α_R values within each study site and black bars indicate ±1 SD. Modified figure from ref. [30]. Circle sizes are proportional to water temperature (as an average during the time of measurement) in each site. Pictures illustrate rivers' characteristic of each biome and show that our sites were mostly open canopy in all biomes.

Isotopic fractionation values. The respiration isotopic fractionation factor (α_R) varies across rivers[30], but rivers are heterogeneous and α_R could also vary within a river. We, therefore, did sensitivity testing on our diel $\delta^{18}O_2$ models using the entire range of values we obtained from site-specific α_R field measurements (Fig. 1) from rivers around the world[30] as well as the specific values of α_R measured at each site. We assume that values from all measurements from all our sites represent reasonable range of values for α_R in rivers and that the most appropriate river-specific α_R value would fall within that range. We selected the α_R that produced the best model fit, measured as the lowest sum of squared differences between observed and modeled $\delta^{18}O_2$ data.

Variation of daytime ecosystem respiration. $\delta^{18}O_2$-ER (ER derived from coupled O_2 and $\delta^{18}O_2$ models that allows ER to vary over 24 h) was consistently higher during the day than at night in all fourteen sites that we sampled (Fig. 2), and substantially greater than ER_{O2} (ER derived from traditional O_2—only models). We found differences in the magnitude of the variation in $\delta^{18}O_2$-ER rates during the day compared to night among sites, with a range of increase throughout the day from about 1 to 113 g O_2 m^{-2} d^{-1} compared to night, depending on site. Some rivers exhibited a similar amplitude of variation in daytime $\delta^{18}O_2$-ER even if they were in different biomes, like the warm turbid Sekong in Cambodia, the cold sub-arctic Corina River in Patagonia, the shallow temperate mountain steppe Lake Creek in the U.S., and the large mountain steppe Eg River (site Eg2) in Mongolia. All these sites had a daytime amplitude of variation in $\delta^{18}O_2$-ER of ~6 g O_2 m^{-2} d^{-1}. Sites with a higher amplitude of variation included the Mekong (daytime amplitude 30 g O_2 m^{-2} d^{-1}), Delgermoron (22 g O_2 m^{-2} d^{-1}), Eg1 (18 g O_2 m^{-2} d^{-1}), Sourdough Creek (20 g O_2 m^{-2} d^{-1}); and a particularly high amplitude of variation in the Mongolian desert sites Zavkhan 1 (113 g O_2 m^{-2} d^{-1}) and Zavkhan 2 (45 g O_2 m^{-2} d^{-1}) (Fig. 2). The mass balance of O_2 in the models requires that GPP increases to offset predicted ER increases obtained from the $\delta^{18}O_2$ portion of

the model. As such, $\delta^{18}O_2$-GPP (GPP derived from coupled O_2 and $\delta^{18}O_2$ models that allow GPP to vary over 24 h) also differed from GPP_{O2}, with substantially greater GPP estimates compared to GPP derived from traditional O_2-only models (Fig. 3).

Isotope models and global underestimates of GPP and ER. When $\delta^{18}O_2$ model results were normalized to 20 °C as in ref. [33] (reported as diel $20\delta^{18}O_2$-ER and $20\delta^{18}O_2$-GPP), diel $20\delta^{18}O_2$-ER and $20\delta^{18}O_2$-GPP remained significantly higher than ER_{O2} and GPP_{O2}, suggesting temperature was not the main driver of variation in daytime $20\delta^{18}O_2$-ER. Mean diel $20\delta^{18}O_2$-ER ranged from 1.5 g O_2 m^{-2} d^{-1} in the Khovd River, to 33.6 g O_2 m^{-2} d^{-1} in the Zavkhan 2 River in the Mongolian desert. In contrast, ER_{O2} from O_2 only ranged from 0.5 to 10.8 g O_2 m^{-2} d^{-1} (Supplementary Table 1). The values of diel $20\delta^{18}O_2$-ER were 1.5 to 22.3-fold higher than ER_{O2} (Fig. 4), but for most sites, $20\delta^{18}O_2$-ER was 2 to 3-fold higher, apart from the tropical Mekong (18-fold higher) and the desert Zavkhan 1 (22-fold higher). $20\delta^{18}O_2$-GPP ranged from 0.66 g O_2 m^{-2} d^{-1} in Khovd River to 24.9 g O_2 m^{-2} d^{-1} in the Zavkhan 2 site in the Mongolian desert compared to 0.01–3.2 g O_2 m^{-2} d^{-1} of GPP_{O2} (Supplementary Table 1). $20\delta^{18}O_2$-GPP values were from 1.1 to 87-fold higher than GPP_{O2} (Fig. 5).

The stepwise multiple regression after variable selection with the lowest Akaike's Information Criterion (AIC) showed that 20 °C temperature-normalized $20\delta^{18}O_2$-ER was best explained by the model (Eq. (1), Supplementary Table 2):

$$20\delta^{18}O_2 - ER = conductivity + \% \text{ of impacted land use} + 20\delta^{18}O_2 - GPP + \text{water depth} \tag{1}$$

which explained 87% of total variance. $20\delta^{18}O_2$-GPP explained 76.7% of total variance in $\delta^{18}O_2$-ER, while conductivity explained 4%, land use 5.6%, and water depth 4.8%. Other parameters included in the initial analyses but not included in the selected model were biofilm ash-free dry mass, water velocity, and slope. These results suggest that factors that could have influenced α_R
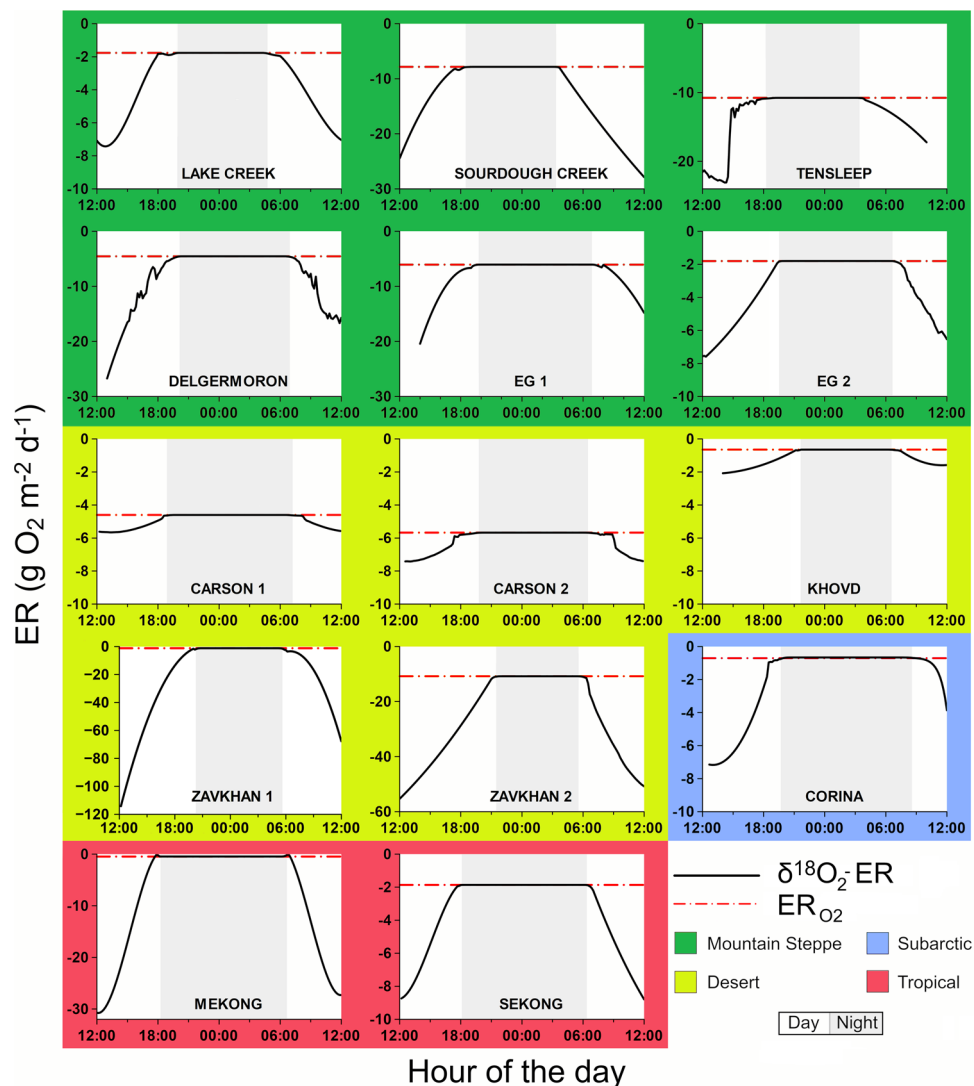
Fig. 2 Diel rates of ecosystem respiration $\delta^{18}O_2$-ER from dual $\delta^{18}O_2$ and O_2 model compared to ER_{O_2} from O_2-only model. Ecosystem respiration (ER) in rivers estimated as diel $\delta^{18}O_2$-ER (solid lines from dual $\delta^{18}O_2$ and O_2 model) compared to ER_{O_2} (dashed red line from the O_2-only model). Green panels represent mountain steppe sites, yellow panels desert sites, and red panels tropical sites. The gray shading represents night hours.
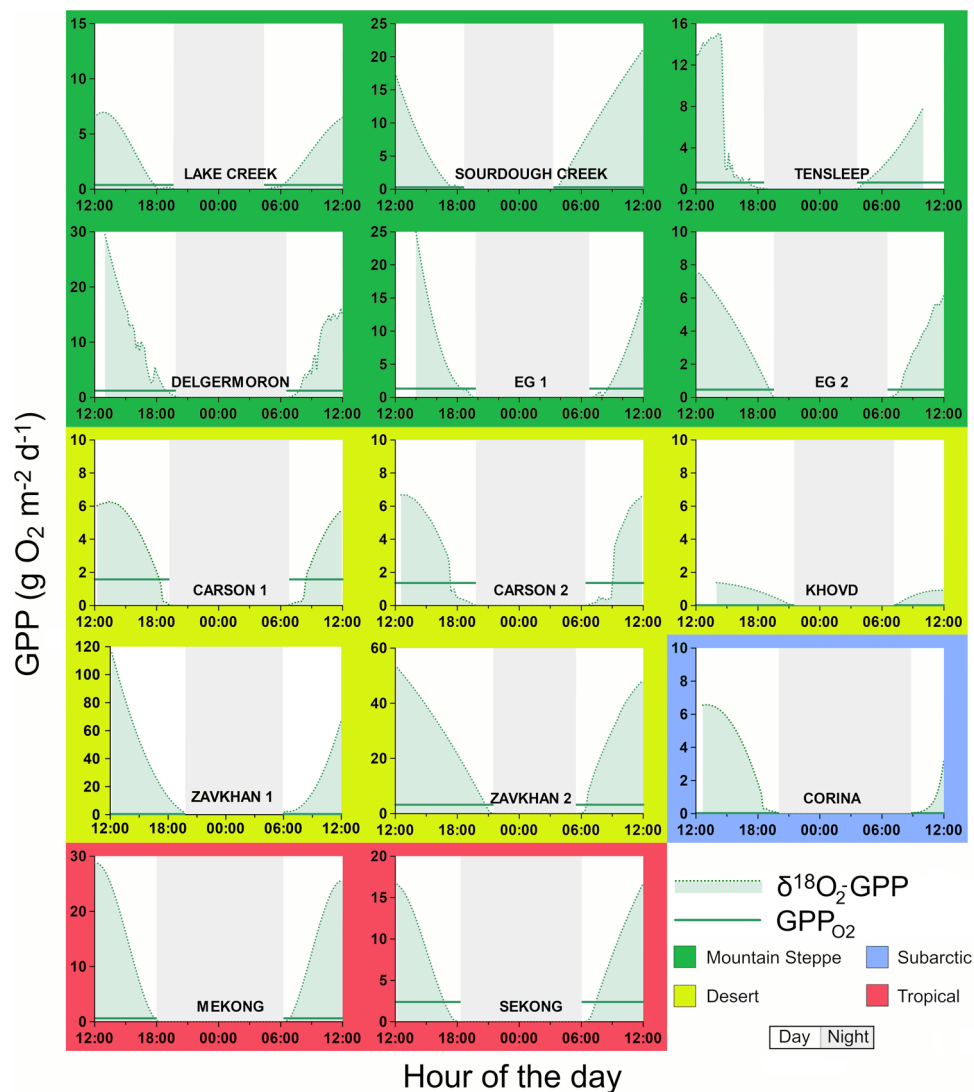
Discussion

Persistent challenges to understanding carbon cycling in aquatic ecosystems include obtaining accurate estimates of carbon fixation and respiration as well as identifying drivers of carbon cycling processes. In this study, we reveal large underestimates of both GPP and ER across rivers from different ecoregions and biomes (tropics, temperate, subarctic) associated with traditional metabolism estimates based on dissolved O_2 concentrations. Further, we found large diel variation in ER that is overlooked in metabolism models that assume constant day-night ER. We show that rivers have substantially higher daytime ER (and GPP) with a coupled modeling approach using diel changes in dissolved O_2 concentration and $\delta^{18}O_2$ values. Our findings hold for all fourteen sites in rivers from tropical, temperate, and subarctic biomes across the globe where we applied the diel model, spanning a broad diversity of productivity, climatic, and physical characteristics (Table 1). Our results demonstrate how oxygen and carbon in rivers potentially cycle much more rapidly over 24-h than

traditional models based only on O_2 concentrations would suggest, and thus highlight how ecosystem scientists potentially underestimate riverine carbon cycling and the importance of primary production in rivers. We found that the differences between ER measured with traditional O_2 metabolism models versus coupled O_2-$\delta^{18}O_2$ models, previously limited to four temperate streams, may be even greater in the tropics (in this study up to 1700%) and in desert rivers in Mongolia (in this study up to 2200%). Our study suggests that streams and rivers globally could be more active in photosynthesizing and respiring carbon than previously estimated.

We found that: (1) the main mechanism driving differences in ER estimates over 24 h was related to the activity of photosynthetic organisms; and (2) that normalizing metabolism estimates to 20 °C did not substantially alter our main results, indicating that photosynthesis was still the main driver of increased ER during the day. These results rule out the idea that high daytime temperatures alone increase daytime ER as influenced by increased metabolic rates as well as diffusion limitation with temperature. In fact, tropical rivers without marked diel temperature variations had just as pronounced diel $\delta^{18}O_2$-ER variation as temperate ecosystems.

and bias our models (e.g., water velocity, ash-free dry mass, water depth) did not influence our final results.

Fig. 3 Diel rates of gross primary production δ¹⁸O₂-GPP from dual δ¹⁸O₂ and O₂ model. Gross primary production (GPP) in rivers estimated as diel δ¹⁸O₂-GPP (green shading from dual δ¹⁸O₂ and O₂ model) compared to GPP$_{O2}$ (green line from O₂–only model). Green panels represent mountain steppe sites, yellow panels desert sites, and red panels tropical sites. The gray shading represents night hours.

The positive relationship between $20\delta^{18}O_2$-ER and $20\delta^{18}O_2$-GPP lends itself to different possible mechanistic explanations. First, increased carbon availability to heterotrophs during the day through leakage of photosynthate stimulates daytime ER. Primary producers can release dissolved organic carbon (DOC) byproducts of photosynthesis that heterotrophs consume rapidly[23,34]. Second, photolysis of organic carbon during daytime could also increase carbon availability to heterotrophs[35]. While we did not directly measure exudation or photolysis in our study, diel changes in metabolism in response to GPP-derived DOC exudation and/or photochemical changes in DOC availability can occur in marine[36], stream[37], and lake[19,38] ecosystems. Short-term $^{13}C_{DIC}$ addition experiments and models confirm rates of newly fixed dissolved organic carbon exudation from photosynthesis[24,39–41]. Carbon exudation by primary producers can also enhance ER over short time scales. Algal respiration rates are boosted 50–140% when algae are exposed to light before a dark measurement as opposed to being held in the dark[42]. Algal carbon is preferentially shunted into riverine food webs[43,44]. Phytoplankton can release up to 60% of their primary production as dissolved organic carbon[45]. This leakage and rapid use by heterotrophic components of biofilms has previously been suggested to fuel high primary production by freeing CO_2 for primary producers based on detailed microelectrode measurements[46].

A third mechanistic explanation could be photorespiration causing oxidation of photosynthate in the cells immediately upon carbon fixation[47]. Photorespiration is an inefficiency of photosynthesis and would have little impact on the rest of the food web or estimates of total carbon flux, as the entire process happens within single cells or organisms. In contrast, if increased GPP-derived DOC exudation and/or photochemical increased DOC availability to the heterotrophic community does occur, then there may be a considerable misunderstanding of how whole-stream metabolism measurements relate to energy transfer into food webs and that we have vastly underestimated the rates of microbial activity and carbon re-cycling in rivers.

We used our data to explore potential contrasting expectations depending upon dominance of photorespiration or temperature-driven changes in ER. Metabolic activity in most flowing waters is dominated by benthic biofilms and sediments[48]. However, little is known about photorespiration in biofilms, as most work on algal photorespiration has been conducted using cultures of marine phytoplankton. Photorespiration is greatest when the ratio of
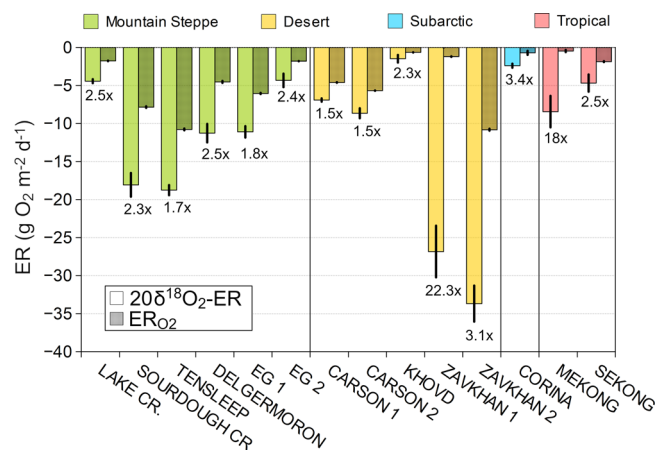
Fig. 4 Temperature normalized (20 °C) diel rates of ecosystem respiration (20δ¹⁸O₂-ER) from dual δ¹⁸O₂ and O₂ model compared to diel ER_O2 rates from O₂-only model. 20δ¹⁸O₂-ER rates from dual δ¹⁸O₂ and O₂ model (solid bars) compared to ER_O2 (patterned bars) estimated with O₂-only metabolism models that assume ER is constant over 24-h. Labels indicate the magnitude of the difference between 20δ¹⁸O₂-ER and ER_O2 for each site. Black bars indicate ±1 SD of posterior model estimates.
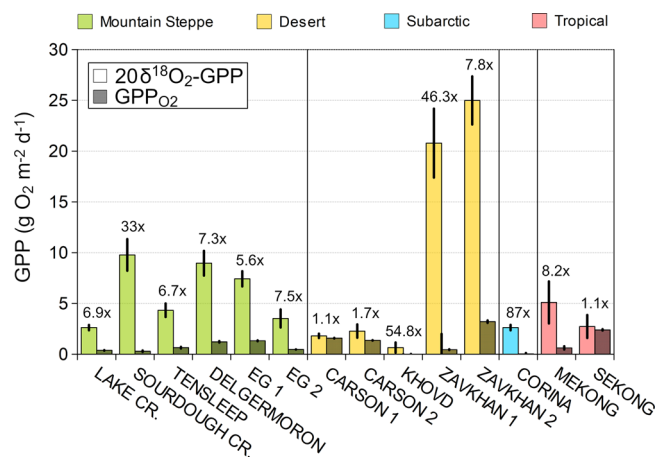
Fig. 5 Temperature normalized (20 °C) diel rates of primary production 20δ¹⁸O₂-GPP from dual δ¹⁸O₂ and O₂ model compared to diel GPP_O2 rates from O₂-only model. 20δ¹⁸O₂-GPP rates from dual δ¹⁸O₂ and O₂ model (solid bars) rates compared to GPP_O2 (patterned bars) estimated with O₂—only metabolism models. Labels indicate the magnitude of the difference between 20δ¹⁸O₂-GPP and GPP_O2 for each site. Black bars indicate ±1 SD of posterior model estimates.

$O_2:CO_2$ is high, and this is accentuated at high light[31] and higher temperatures[32]. Not all species of algae exhibit photorespiration[47]. Limitation of CO_2 and concurrent O_2 increases with photosynthesis in rivers leading to $O_2:CO_2$ that increases during the day, peaking a few hours after noon[49]. Thus, we expect peak photorespiration to lag behind maximum light because of temperature increases and $O_2:CO_2$ continuing to increase following the maximum light as indicated by ER. If temperature stimulates ER rates, then a time lag of ER after the peak light could solely be related to temperature dependence of ER. The temperature-normalized 20δ¹⁸O₂-ER peaked before maximum light in six rivers and at maximum light in eight rivers (Supplementary Figs. 2, 3, and 4). Vertical structure of biofilms with steep light attenuation and tight association with heterotrophic components alters the predictions of when photorespiration will dominate. High heterotrophic activity will

decrease $O_2:CO_2$, discouraging photorespiration. High O_2 stimulates photorespiration in cyanobacterial biofilms, but photosynthesis deeper in the mat under lower light still dominates net production of the mat[46]. Similar steep light gradients occur in river periphyton, and as light intensity increases, deeper portions of the mat have more active photosynthesis[50]. These deeper portions of the mat are in conditions less conducive to photorespiration. In summary, our data exploration, combined with the fact that not all primary producers exhibit photorespiration and deeper biofilm photosynthesis may reduce photorespiration, suggests that photorespiration is not the main explanation for high ER rates during the day.

It is likely that some of the enhanced ER during the daytime is attributable to carbon released and respired by heterotrophic organisms over short time periods. However, our measurements cannot rule out photorespiration even though we suggest it is not likely to be the main driver of higher daytime ER estimated using δ¹⁸O₂ (see above discussion). If a substantial portion of carbon enters the microbial loop and fuels high daytime ER, there could be implications for biogeochemical processes that influence water quality and gas release from streams (e.g., denitrification and methanogenesis) even if the mass balance of O_2 and NEP does not change. Our results also suggest further studies quantifying ER during the day, as well as tests of the potential mechanisms driving higher daytime ER in freshwater ecosystems, are warranted. These could include additional models of daytime ER incorporating simultaneous measurements of DIC concentration and DIC- δ¹³C, together with δ¹⁸O₂. Pulse-chase isotope experiments[24] could also potentially identify pathways of carbon fixation, release from primary producers to heterotrophs, and fate at the scale of whole ecosystems.

Some of our δ¹⁸O₂ model estimates of diel ER were more uncertain (e.g., error bars in Figs. 4 and 5, Supplementary Fig. 5), pointing to ongoing challenges associated with diel δ¹⁸O₂ metabolism models, especially for rivers with low GPP and high rates of air-water gas exchange. When physical processes mask biological signals in diel O_2 and δ¹⁸O₂, we have less certain estimates of ER and GPP. A higher level of uncertainty of the diel δ¹⁸O₂ model also derives from the limited amount of δ¹⁸O₂ data obtained by grab samples every 2 h, compared to models derived from high-frequency 10-min O_2 data from sensors. Technologies able to simultaneously collect O_2 concentration and δ¹⁸O₂ at similarly high frequency (e.g., field-deployable spectroscopic analyzers of δ¹⁸O₂[51]) and over several days could improve model fits compared to those derived from a reduced number of diel δ¹⁸O₂ samples. We assessed the level of uncertainty of our models based on the minimum value of the sum of squared differences of modeled versus observed O_2 concentrations and δ¹⁸O₂ values (Supplementary Table 1). However, even after consideration of some level of uncertainty, the δ¹⁸O₂-ER and Gδ¹⁸O₂-GPP estimates were significantly higher than ER_O2 and GPP_O2 estimates in all biomes (error bars reported in Figs. 4 and 5). Further research and model development will better constrain model estimates and assess the processes that are driving large diel variations in GPP and ER.

Our model fits were based on the respiration isotopic fractionation factor, α_R, that produced the best model fits (i.e., minimum sum of squared difference between observed and modeled δ¹⁸O₂ data) within a range of possible α_R values that we measured in rivers across the globe[30]. Even if the α_R is difficult to establish for a river community at the ecosystem scale, it can be estimated within a reasonable range (in our study the range of measured α_R in rivers globally[30]) and here we constrained estimates by the best model fit of 24-h diel δ¹⁸O₂ data. In most of our study rivers, the α_R values that produced the best model fits were in the lower range of measured α_R values (0.997–0.999), and the associated δ¹⁸O₂-ER values were also in the lower range in those sites.

Table 1 Summary of site locations and characteristics in different biomes (temperate, tropical, and sub-arctic[63]) and ecoregions (mountain steppe, desert[64]).

River name	Date dd/mm/yy	State Country	Lat/Long	Biome/ Ecoregion	Discharge m³/s	Impacted Land-Use %	Average Temperature °C
Lake Creek	16/7/2017	Wyoming USA	44.18883/ −107.2118	Temperate/ Mountain steppe	0.33	0	14.6
Sourdough Creek	14/7/2017	Wyoming USA	44.24602/ −106.96013	Temperate/ Mountain steppe	0.37	0	10.2
Tensleep	11/7/2017	Wyoming USA	44.24605/ −107.22325	Temperate/ Mountain steppe	2.57	0	16.2
Delgermörön	9/9/2017	Khovsgol Mongolia	50.17575/ 98.48293	Temperate/ Mountain steppe	0.92	2	8.4
Égjin gol (Eg)1	22/9/2017	Bulgan Mongolia	50.09532/ 101.59291	Temperate/ Mountain steppe	0.43	0	5.1
Égjin gol (Eg) 2	15/9/2017	Bulgan Mongolia	50.56733/ 101.52973	Temperate/ Mountain steppe	7.62	1	9.6
Carson 1 Lower watershed	15/9/2018	Nevada USA	39.28950/ −119.29102	Temperate/Desert	0.4	8	16.7
Carson 2 Upper watershed	25/8/2018	Nevada USA	38.68235/ −119.93011	Temperate/Desert	0.039	0	13.9
Khovd	6/8/2018	Khovd Mongolia	49.18462/ 89.29811	Temperate/Desert	2.95	26	15.5
Zavkhan 1 Lower watershed	26/7/2018	Zavkhan Mongolia	48.27917/ 93.48121	Temperate/Desert	11.99	1	20.1
Zavkhan 2 Upper watershed	22/7/2018	Zavkhan Mongolia	47.08973/ 97.53291	Temperate/Desert	10.16	49	14.5
Corina	18/3/2018	Patagonia	−47.2808333/ 72.6286111	Subarctic	0.6851	22	7.6
Mekong	18/1/2018	Cambodia	11.7069444/ 104.9730556	Tropical	5,550	56	26.0
Sekong	23/1/2018	Cambodia	13.607669/ 106.096223	Tropical	382	38	27.3

In summary, we found that ignoring differences in day versus night ecosystem metabolism could lead to a potentially large mischaracterization of metabolic processes occurring within rivers. Our study suggests that many streams and rivers photosynthesize and respire carbon much faster than traditional metabolism models predict and that we are currently underestimating carbon cycling within rivers (which is likely dominated by the microbial loop and benthic processes). Insights about diel metabolism patterns from streams and rivers are relevant to other benthic biofilm-dominated ecosystems (e.g., ponds, wetlands, shallow lakes, reefs, estuaries), which may have similarly higher daytime GPP and ER than O_2- or CO_2-only models can predict. Based on the relationship we found between GPP and ER estimated using results from our coupled model of O_2 and $\delta^{18}O_2$, photosynthesis occurring during the day likely stimulates daytime heterotrophic microbial activity through organic carbon exudation by primary producers. Our results indicate that photosynthesis can be substantially more important to river and stream food webs than previously thought. Finally, because researchers traditionally use diel O_2 concentration methods to investigate the processes in rivers that generate carbon dioxide, such mischaracterization could limit our ability to understand mechanistically what is driving carbon dioxide flux and extrapolating local controls to global processes. Future research elucidating the coupled processes that fix and respire carbon on very short time scales, and how these may change with ongoing human alterations of flow regimes, eutrophication, climate change are critical next steps for an improved understanding of the magnitude and drivers of ecosystem metabolism in streams and rivers.

Methods

Study sites and data collection. During 2017 and 2018, we carried out 14 experiments in rivers located in temperate, tropical, and subarctic biomes to capture a gradient of river productivity and climatic characteristics (Table 1, Fig. 1). Apart from the Mekong and Sekong rivers in Cambodia that were impacted by plantations, rice cultivation, grassland, and urban areas (56% impacted land cover in the Mekong and 38% in the Sekong), the selected rivers were predominantly in pristine areas (impacted land-use ≤ 8%), although two rivers in Mongolia were affected by livestock grazing (with 26% of land cover at the Khovd and 59% in the two Zavkhan rivers).

We conducted traditional O_2 concentration metabolic assessments, assessments of isotopic fractionation, and 24 h characterization of $\delta^{18}O_2$ at each site. We measured changes in dissolved O_2 concentrations and temperature every 10 min over at least 24 h with at least one MiniDOT logger (PME, Vista, California, USA). We calibrated for drift using the average measurement values made in 100% saturated water for at least 30 min before and after each deployment to allow adjustment to temperature and placed sensors in the river for at least 30 min prior to using data to allow equilibration to temperature (following methods detailed in ref. [52]).

We collected $\delta^{18}O_2$ samples by hand every 2 h during the same 24-h period of the O_2 concentration measurements in pre-evacuated 100 mL vials loaded with 50 µl $HgCl_2$ as a preservative and sealed with septum stoppers (Bellco Glass Inc., Supelco, Vineland NJ). We analyzed samples for $\delta^{18}O_2$ at the Nevada Stable Isotope Lab of the University of Nevada, Reno with a Micromass Isoprime (Middlewich, UK) stable isotope ratio mass spectrometer. We followed the method described by ref. [17] and injected 1.0–2.5 mL of headspace gas taken from the serum bottles using a gastight syringe (SGE, Australia) into a Eurovector (Pavia, Italy) elemental analyzer equipped with a septum injector port, and a 1.5 m long molecular sieve gas chromatography column. Water-$\delta^{18}O$ was also collected at each site every 2 h and analyses were performed using a Picarro L2130-i cavity ringdown spectrometer at the Nevada Stable Isotope Lab of the University of Nevada, Reno. $\delta^{18}O_2$ values are reported in the usual δ notation vs. VSMOW in units of ‰, with an analytical uncertainty of ±0.2‰ for $\delta^{18}O_2$, or an analytical uncertainty of ±0.1‰ for water-$\delta^{18}O$.

We characterized physical characteristics at each site to provide parameters to estimate whole-system metabolism. We measured conductivity, slope, and flow velocity and depth at ten transects using a flow meter when wadeable or with an Acoustic Doppler Velocimeter (Sontek, Xylem, San Diego, CA) when rivers were not wadeable. At each site, we measured light as photosynthetically active radiation (PAR) every 10 min, using Odyssey PAR loggers (Data Flow Systems, Christchurch, New Zealand) calibrated with a Li-Cor PAR sensor (Lincoln, Nebraska, USA).

At each site, we also directly measured biofilm ash-free dry mass (AFDM) from 8 to 12 rocks ([53]). The material was scrubbed from the rocks, agitated, filtered

(Whatman glass microfiber GF/F filters). Rock area was estimated with calibrated pictures processed with the ImageJ processing program (National Institutes of Health and the Laboratory for Optical and Computational Instrumentation LOCI, University of Wisconsin). For AFDM analyses, samples were dried, and weighed before and after combustion.

Additionally, we collected data on the percentage of impacted land use in the watershed above each sampling site: for the Mekong and the Sekong we used Landsat satellite imagery from ref. [54], for the US and Mongolian sites land use characteristics were derived from the National Land Cover Database[55] and for Patagonia we used the Chilean national land use inventory maps from ref. [56].

$\delta^{18}O_2$ stable isotope fractionation during respiration in sealed recirculating chambers. Models based on oxygen isotopes are sensitive to the oxygen isotope fractionation factor (α_R) during respiration used; α_R can vary widely among sites and is influenced by temperature and water velocity[30]. We used in our models the range of α_R values measured by[30] using sealed Plexiglas recirculating chambers as in ref. [57]. These measurements were done at the same time as the 24 h $\delta^{18}O_2$ sample collections in the rivers of this study. We placed rocks, sediment, macrophytes (macrophytes dominated in the Zavkhan 1 site) inside the chambers, depending on the site's dominant substrata (see ref. [30] for more details on chamber measurements). We collected water samples in the chambers for $\delta^{18}O_2$ analyses before and after the incubations and the O_2 isotope fractionation factor was calculated using Eq. (2).

$$\delta = (\delta i + 1000)F^{(\alpha-1)} - 1000 \quad (2)$$

where δ is the O_2 isotopic composition of dissolved oxygen at the end of the dark incubation, δ_i is the O_2 isotopic composition of dissolved oxygen at the beginning of the dark incubation, F the fractional abundance of O_2 concentration remaining at the end of the dark incubation, and α is the isotopic fractionation factor during respiration.

Ecosystem metabolism O_2 single station modeling. We modeled metabolism as a function of GPP, ER, and reaeration with the atmosphere, using the single-station open-channel metabolism method[4] using the same approach as[15], given in Eq. (3).

$$O_{2_{(t)}} = O_{2_{(t-1)}} + \left(\left(\frac{GPP}{z} x \frac{PPFD_{(t-1)}}{\sum PPFD_{24h}} \right) + \frac{ER}{z} + K_{O_2}\left(O_{2_{sat(t-1)}} - O_{2_{(t-1)}} \right) \right) \triangle t \quad (3)$$

where GPP is gross primary production in g O_2 m^{-2} d^{-1}, ER is ecosystem respiration in g O_2 m^{-2} d^{-1}, K_{O_2} is the reaeration coefficient (d^{-1}). PPFD is photosynthetic photon flux density (µmol m^{-2} s^{-1}), z is mean stream depth (m), and Δt is time increment between logging intervals (d). We used Bayesian inverse modeling approach to estimate the probability distribution of parameters GPP and ER that produce the best model fit between observed and modeled O_2 data. We fixed site-specific K_{O_2} estimates using K600 (d^{-1}) (normalized beyond gas-specific Schmidt number conversions among gases[58]) based on prior work characterizing K using BASE[59], and converted these prior estimates of K600 to K_{O_2} using appropriate temperature corrections. We estimated daily GPP and ER from diel O_2 data only (Eq. (3)) to be used as prior estimates of daily GPP_{O_2} and ER_{O_2} in the coupled O_2 and $\delta^{18}O_2$ model (Eqs. (4a) and (4b))[15], where the mean and SD of GPP and ER from the O_2 –only method were used as prior estimates of GPP_{O_2} and ER_{O_2} in the dual O_2 and $\delta^{18}O_2$ model described below.

Ecosystem metabolism: Diel $\delta^{18}O_2$ modeling. We also modeled metabolism using an updated version of the model developed by ref. [15] coupling high-frequency O_2 concentration data with $\delta^{18}O_2$ collected every 2 h throughout the same 24 h period of the O_2 concentration measurements. With this model, daily rates of ecosystem metabolism are derived from diel changes in $\delta^{18}O_2$ and O_2, where values of $\delta^{18}O_2$ are converted to g ^{18}O m^{-3} ($^{18}O_2$ in Eq. 4b) and modeled as a function of water isotope values, isotope fractionation, reaeration with the atmosphere, ER, and GPP. As with Eq. 3, the ratio of light at the previous logging time ($PPFD_{(t-1)}$) relative to the sum of light over 24 h ($\sum PPFD_{24h}$) is used to characterize times when GPP is zero and only ER is taking place (Eqs. (4a) and (4b)):

$$O_{2_{(t)}} = O_{2_{(t-1)}} + \left(\frac{GPP_{O2}}{z} x \frac{PPFD_{(t-1)}}{\sum PPFD_{24h}} \right) + \left(\frac{ER_{O2} x \triangle t}{z} \right)$$
$$+ \left(K_{O_2} x \left(O_{2_{sat(t-1)}} - O_{2_{(t-1)}} \right) x \triangle t \right) \quad (4a)$$

$$^{18}O_{2_{(t)}} = {}^{18}O_{2_{(t-1)}} + \left(\frac{(GPP_{O2} + dielMET)}{z} x \frac{PPFD_{(t-1)}}{\sum PPFD_{24h}} x \alpha_P x AF_W \right)$$
$$+ \left(\frac{ER_{O2} x \triangle t}{z} x \alpha_R x AF_{DO}(t-1) \right)$$
$$+ \left(\frac{(-dielMET)}{z} x \frac{PPFD_{(t-1)}}{\sum PPFD_{24h}} x \alpha_R x AF_{DO}(t-1) \right)$$
$$+ \left(K_{O_2} x \alpha_g x \triangle t x \left(\left(O_{2_{sat(t-1)}} x \alpha_g x AF_{atm} \right) - {}^{18}O_{2_{(t-1)}} \right) \right) \quad (4b)$$

Where GPP_{O2} and ER_{O2} (g O_2 m^{-2} d^{-1}) refer to the values obtained from diel O_2

only, dielMET (g O_2 m^{-2} d^{-1}) is the diel metabolism term that allows for the estimation of diel ER and GPP from $^{18}O_2$, K_{O_2} is the O_2 gas exchange rate (d^{-1}), z is mean stream depth (m), PPFD is photosynthetic photon flux density (μmol m^{-2} s^{-1}), Δt is time step between measurements (d), $^{18}O_2$ is the concentration of ^{18}O in dissolved O_2 (g ^{18}O m^{-3}), AF$_{DO}$ is atomic fraction of dissolved O_2 (mol^{18}O:mol O_2, measured), AF$_w$ is atomic fraction of H_2O (mol ^{18}O:mol O_2, measured), AF$_{atm}$ is atomic fraction of atmospheric air (mol^{18}O:mol O_2, literature), α_g is the fractionation factor during air–water gas exchange (0.9972, from ref.[60]), α_R is the fractionation factor during respiration measured in the chambers (varied by site[30]; Fig. 1), α_p is the fractionation factor during photosynthesis (1.0000 from ref.[60]).

The inverse modeling approach finds the best estimates of parameters to match measured and modeled dissolved O_2. The model assumes that the measured changes in O_2 concentration represent the actual net diel changes in O_2 concentration and uses an additional parameter, dielMET, that is a function of the isotopic enrichment occurring during respiration, derived from diel $^{18}O_2$. This parameter increases daily ER$_{O_2}$ and GPP$_{O_2}$ of the same amount, adding and subtracting dielMET, to obtain daily $\delta^{18}O_2$.ER and $\delta^{18}O_2$-GPP, respectively.

We estimated the posterior distributions of unknown parameters (ER$_{O_2}$, GPP$_{O_2}$, and dielMET) using a Bayesian inverse modeling approach[15] and Markov chain Monte Carlo sampling with the R *metrop* function in the *mcmc* package[61,62]. Each model was run for at least 200,000 iterations using nominally informative priors based on the range of ER$_{O_2}$ and GPP$_{O_2}$. For dielMET, we used a minimally informative uniform prior distribution (0–100 g O_2 m^{-2} d^{-1}). We removed the first 10,000 iterations of model burn-in and assessed quality of model fit. Model runs using the minimum, average, and maximum α_R values measured in the field recirculating chambers were also compared, and we selected the α_R and report associated model metabolism estimates that generated the lowest sum of squared differences between the observed and modeled O_2 and $^{18}O_2$ diel values.

Temperature-normalized comparisons. To test the effect of temperature from the daily $\delta^{18}O_2$-ER and $\delta^{18}O_2$-GPP rates and account for daily variations in temperature, we normalized estimates from models to 20 °C (and report them as 20$\delta^{18}O_2$-ER and 20$\delta^{18}O_2$-GPP) for comparison with O_2-derived metabolism estimates following[33] with Eq. (5):

$$rate\ at\ 20\,^{\circ}C = \frac{2.523 * e^{(0.0552*20)}}{2.523 * e^{(0.0552*t_1)}} * rate\ at\ t_1 \tag{5}$$

Where t_1 is site temperature and rate is the measured rate (i.e., GPP or ER) at t_1.

Statistical analyses. We used multiple linear regression to find the best predictor of the magnitude of diel 20$\delta^{18}O_2$-ER and differences between sites. To select the best model, we performed a stepwise variable selection and selected the best model based on the lowest AIC. Tested variables included percentage of impacted land use (%), 20$\delta^{18}O_2$-GPP (g O_2 m^{-2} d^{-1}), conductivity (μS/cm), ash-free dry mass (AFDM, g), slope (%), water depth (m), and flow velocity (m/s) measured in the field. We used ANOVA to test the relative contribution of each variable selected with the AIC to total variance. Analyses were run with the R software[61].

Reporting summary. Further information on research design is available in the Nature Portfolio Reporting Summary linked to this article.

Data availability

The data sets (MacroRivers_AllData_AllSites; https://doi.org/10.6084/m9.figshare.20134997) that support the findings of this study are available in Figshare Digital Repository https://figshare.com.

Code availability

The R code used to generate the results of this study is available from the corresponding author upon reasonable request.

References

1. Cole, J. J. et al. Plumbing the global carbon cycle: integrating inland waters into the terrestrial carbon budget. *Ecosystems* **10**, 171–184 (2007).
2. Battin, T. J. et al. Biophysical controls on organic carbon fluxes in fluvial networks. *Nature Geosci.* **1**, 95–100 (2008).
3. Raymond, P. A. et al. Global carbon dioxide emissions from inland waters. *Nature* **503**, 355–359 (2013).
4. Odum, H. T. Primary production in flowing waters. *Limnol. Oceanogr.* **1**, 102–117 (1956).
5. Appling, A. P. et al. The metabolic regimes of 356 rivers in the United States. *Scientific Data* **5**, 180292 (2018).
6. O'Donnell, B. & Hotchkiss, E. R. Resistance and resilience of stream metabolism to high flow disturbances. *Biogeosci. Discuss.* **2020**, 1–36 (2020).
7. Gómez-Gener, L., Lupon, A., Laudon, H. & Sponseller, R. A. Drought alters the biogeochemistry of boreal stream networks. *Nat. Commun.* **11**, 1795 (2020).
8. Saltarelli, W. A. et al. Variation of stream metabolism along a tropical environmental gradient: Stream metabolism variation. *J. Limnol.* **77**, (2018).
9. Dodds, W. K. et al. The freshwater biome gradient framework: predicting macroscale properties based on latitude, altitude, and precipitation. *Ecosphere* **10**, e02786 (2019).
10. Hall, R. O., Hotchkiss, E. R. Stream metabolism. in *Methods in Stream Ecology* 3rd edn, Vol. 2, (eds Hauer, F. R. & Lamberti, G. A.) (Academic Press, 2017).
11. Mader, M., Schmidt, C., van Geldern, R. & Barth, J. A. C. Dissolved oxygen in water and its stable isotope effects: a review. *Chem. Geol.* **473**, 10–21 (2017).
12. Luz, B. & Barkan, E. Assessment of oceanic productivity with the triple-isotope composition of dissolved oxygen. *Science* **288**, 2028–2031 (2000).
13. Tobias, C. R., Böhlke, J. K. & Harvey, J. W. The oxygen-18 isotope approach for measuring aquatic metabolism in high-productivity waters. *Limnol. Oceanogr.* **52**, 1439–1453 (2007).
14. Holtgrieve, G. W., Schindler, D. E., Branch, T. A. & A'mar, Z. T. Simultaneous quantification of aquatic ecosystem metabolism and reaeration using a Bayesian statistical model of oxygen dynamics. *Limnol. Oceanogr.* **55**, 1047–1062 (2010).
15. Hotchkiss, E. R. & Hall, R. O. Jr High rates of daytime respiration in three streams: use of d 18 OO2 and O2 to model diel ecosystem metabolism. *Limnol. Oceanogr.* **59**, 798–810 (2014).
16. Parker, S. R., Poulson, S. R., Smith, M. G., Weyer, C. L. & Bates, K. M. Temporal variability in the concentration and stable carbon isotope composition of dissolved inorganic and organic carbon in Two Montana, USA Rivers. *Aquatic Geochemistry* **16**, 61–84 (2010).
17. Gammons, C., Babcock, J. N., Parker, S. R. & Poulson, S. Diel cycling and stable isotopes of dissolved oxygen, dissolved inorganic carbon, and nitrogenous species in a stream receiving treated municipal sewage. *Chem. Geol.* **283**, 44–55 (2010).
18. Venkiteswaran, J. J., Schiff, S. L. & Wassenaar, L. Aquatic metabolism and ecosystem health assessment using dissolved O_2 stable isotope diel curves. *Ecol. Appl.* **18**, 965–982 (2008).
19. Sadro, S., Nelson, C. E. & Melack, J. M. Linking diel patterns in community respiration to bacterioplankton in an oligotrophic high-elevation lake. *Limnol. Oceanogr.* **56**, 540–550 (2011).
20. Bender, M. et al. A comparison of four methods for determining planktonic community production. *Limnol. Oceanogr.* **32**, 1085–1098 (1987).
21. Bernot, M. J. et al. Inter-regional comparison of land-use effects on stream metabolism. *Freshwater Biol.* **55**, 1874–1890 (2010).
22. Hall, R. O., Tank, J. L., Baker, M. A., Rosi-Marshall, E. J. & Hotchkiss, E. R. Metabolism, gas exchange, and carbon spiraling in rivers. *Ecosystems* **19**, 73–86 (2016).
23. Baines, S. B. & Pace, M. L. The production of dissolved organic matter by phytoplankton and its importance to bacteria: Patterns across marine and freshwater systems. *Limnol. Oceanogr.* **36**, 1078–1090 (1991).
24. Hotchkiss, E. R. & Hall, R. O. Whole-stream 13C tracer addition reveals distinct fates of newly fixed carbon. *Ecology* **96**, 403–416 (2015).
25. Cole, J. J., Likens, G. E. & Strayer, D. L. Photosynthetically produced dissolved organic carbon: an important carbon source for planktonic bacteria1. *Limnol. Oceanogr.* **27**, 1080–1090 (1982).
26. Farjalla, V. F. et al. Influence of hydrological pulse on bacterial growth and DOC uptake in a clear-water Amazonian lake. *Microb. Ecol.* **52**, 334–344 (2006).
27. Perkins, D. M. et al. Consistent temperature dependence of respiration across ecosystems contrasting in thermal history. *Global Change Biol.* **18**, 1300–1311 (2012).
28. Riley, A. J. & Dodds, W. K. Whole-stream metabolism: strategies for measuring and modeling diel trends of dissolved oxygen. *Freshwater Sci.* **32**, 56–69 (2012).
29. Finlay, J. C., Power, M. E. & Cabana, G. Effects of water velocity on algal carbon isotope ratios: implications for river food web studies. *Limnol. Oceanogr.* **44**, 1198–1203 (1999).
30. Tromboni, F. et al. Respiration in rivers fractionates stable isotopes of dissolved oxygen; a global investigation on the influences of temperature and flow. *Biogeochemistry* **147**, 199–210 (2020).
31. Pope, D. H. Effects of light intensity, oxygen concentration, and carbon dioxide concentration on photosynthesis in algae. *Microb. Ecol.* **2**, 1–16 (1975).
32. Davison, I. R. Environmental effects on algal photosynthesis: temperature. *J. Phycol.* **27**, 2–8 (1991).

33. Song, C. et al. Continental-scale decrease in net primary productivity in streams due to climate warming. *Nat. Geosci.* **11**, 415–420 (2018).
34. Kritzberg, E. S., Cole, J. J., Pace, M. M. & Graneli, W. Does autochthonous primary production drive variability in bacterial metabolism and growth efficiency in lakes dominated by terrestrial C inputs? *Aquat. Microb. Ecol.* **38**, 103–111 (2005).
35. Cory, R. M. & Kling, G. W. Interactions between sunlight and microorganisms influence dissolved organic matter degradation along the aquatic continuum. *Limnol. Oceanogr. Lett.* **3**, 102–116 (2018).
36. Rost, B., Riebesell, U. & Sültemeyer, D. Carbon acquisition of marine phytoplankton: Effect of photoperiod length. *Limnol. Oceanogr.* **51**, 12–20 (2006).
37. Schindler, D. E., Jankowski, K., A'mar, Z. T. & Holtgrieve, G. W. Two-stage metabolism inferred from diel oxygen dynamics in aquatic ecosystems. *Ecosphere* **8**, e01867 (2017).
38. Solomon, C. T. et al. Ecosystem respiration: drivers of daily variability and background respiration in lakes around the globe. *Limnol. Oceanogr.* **58**, 849–866 (2013).
39. Bjørrisen, P. K. Phytoplankton exudation of organic matter: why do healthy cells do it? *Limnol. Oceanogr.* **33**, 151–154 (1988).
40. Bade, D. L. et al. Sources and fates of dissolved organic carbon in lakes as determined by whole-lake carbon isotope additions. *Biogeochemistry* **84**, 115–129 (2007).
41. Lyon, D. & Ziegler, S. Carbon cycling within epilithic biofilm communities across a nutrient gradient of freshwater streams. *Limnol. Oceanogr.* **54**, 439–449 (2009).
42. Beardall, J. et al. Studies on enhanced post-illumination respiration in microalgae. *J. Plankton Res.* **16**, 1401–1410 (1994).
43. Pingram, M. A., Collier, K. J., Hamilton, D. P., David, B. O. & Hicks, B. J. Carbon sources supporting large river food webs: a review of ecological theories and evidence from stable isotopes. *Freshwater Rev.* **5**, 85–103.119 (2012).
44. Arsenault, E. R. et al. Intercontinental analysis of temperate steppe stream food webs reveals consistent autochthonous support of fishes. *Ecology Lett.* 1–13 https://doi.org/10.1111/ele.14113 (2022).
45. Myklestad, S. M. Dissolved organic carbon from phytoplankton. In *Marine Chemistry* (ed. Wangersky, P. J.) Springer Berlin Heidelberg (2000).
46. Kühl, M., Glud, R. N., Ploug, H. & Ramsing, N. B. Microenvironmental control of photosynthesis and photosynthesis-coupled respiration in an epilithic cyanobacterial biofilm. *J. Phycol.* **32**, 799–812 (1996).
47. Brendan, C. B., Coleman, J. R. & Colman, B. Measurement of photorespiration in algae. *Plant Physiol.* **69**, 259–262 (1982).
48. Battin, T. J., Besemer, K., Bengtsson, M. M., Romani, A. M. & Packmann, A. I. The ecology and biogeochemistry of stream biofilms. *Nat. Rev. Microbiol.* **14**, 251–263 (2016).
49. Aho, K. S., Hosen, J. D., Logozzo, L. A., McGillis, W. R. & Raymond, P. A. Highest rates of gross primary productivity maintained despite CO_2 depletion in a temperate river network. *Limnol. Oceanogr. Lett.* **6**, 200–206 (2021).
50. Dodds, W. K., Biggs, B. J. F. & Lowe, R. L. Photosynthesis-irradiance patterns in benthic microalgae: variations as a function of assemblage thickness and community structure. *J. Phycol.* **35**, 42–53 (1999).
51. Berhanu, T. A. et al. High-precision atmospheric oxygen measurement comparisons between a newly built CRDS analyzer and existing measurement techniques. *Atmos. Meas. Tech.* **12**, 6803–6826 (2019).
52. Schechner, A. E., Dodds, W. K., Tromboni, F., Chandra, S. & Maasri, A. How do methodological choices influence estimation of river metabolism? *Limnol. Oceanogr. Methods* **19**, 659–672 (2021).
53. Hutchens, J. J. Jr, Wallace, J. B., & Grubaugh, J. W. Transport and storage of fine particulate organic matter. In *Methods in Stream Ecology* (eds G. Lamberti & F. R. Hauer) 37–53 (Elsevier, 2017).
54. Lohani, S., Dilts, T. E., Weisberg, P. J., Null, S. E. & Hogan, Z. S. Rapidly accelerating deforestation in Cambodia's Mekong River Basin: a comparative analysis of spatial patterns and drivers. *Water* **12**, 2191 (2020).
55. Maasri, A. et al. Valley-scale hydrogeomorphology drives river fish assemblage variation in Mongolia. *Ecol. Evolut.* **11**, 6527–6535 (2021).
56. Astorga, A., Moreno, P. C. & Reid, B. Watersheds and trees fall together: an analysis of intact forested watersheds in Southern Patagonia (41–56° S). *Forests* **9**, 385 (2018).
57. Rüegg, J., Brant, J. D., Larson, D. M., Trentman, M. T. & Dodds, W. K. A portable, modular, self-contained recirculating chamber to measure benthic processes under controlled water velocity. *Freshwater Sci.* **34**, 831–844 (2015).
58. Jähne, B. et al. On the parameters influencing air-water gas exchange. *J. Geophys. Res. Oceans* **92**, 1937–1949 (1987).
59. Grace, M. R. et al. Fast processing of diel oxygen curves: estimating stream metabolism with BASE (BAyesian Single-station Estimation). *Limnol. Oceanogr. Methods* **13**, e10011 (2015).
60. Benson, B. B. & Krause, D. Jr The concentration and isotopic fractionation of oxygen dissolved in freshwater and seawater in equilibrium with the atmosphere1. *Limnol. Oceanogr.* **29**, 620–632 (1984).
61. R Core Team. R: A Language and Environment for Statistical Computing. R.F.F.S. Computing, Vienna, Austria, (2012).
62. Geyer, C. J. & Johnson. L. T. mcmc: Markov Chain Monte Carlo. R package version 0.9−2. http://cran.r-project.org/package5mcmc. (2013).
63. Köppen, W. Die Wärmezonen der Erde, nach der Dauer der heissen, gemässigten und kalten Zeit und nach der Wirkung der Wärme auf die organische Welt betrachtet (The thermal zones of the Earth according to the duration of hot, moderate and cold periods and of the impact of heat on the organic world). *Meteorol. Z.* **1**, 215–226 (1884).
64. Holdridge, L. R. Determination of world plant formations from simple climatic data. *Science* **105**, 367–368 (1947).

Acknowledgements

Author contributions

F.T., A.E.S., W.K.D., S.C. carried out fieldwork. F.T. and S.R.P. performed isotope analyses. F.T., E.R.H., and A.E.S. analyzed the data. F.T. performed statistical analyses, generated all figures, and wrote the initial version of the paper. All co-authors contributed to interpreting and discussing the results and developing the paper.

Competing interests

The authors declare no competing interests.

Additional information

Supplementary information The online version contains supplementary material available at https://doi.org/10.1038/s43247-022-00607-2.

Correspondence and requests for materials should be addressed to Flavia Tromboni.

Peer review information *Communications Earth & Environment* thanks Joshua Dean for their contribution to the peer review of this work. Primary Handling Editors: Clare Davis. Peer reviewer reports are available.

Reprints and permission information is available at http://www.nature.com/reprints

Publisher's note Springer Nature remains neutral with regard to jurisdictional claims in published maps and institutional affiliations.